

Effect of Supramolecular Structures on Thermoplastic Zein–Lignin Bionanocomposites

Maria Oliviero,[†] Letizia Verdolotti,[†] Ernesto Di Maio,^{*,§} Marco Aurilia,[#] and Salvatore Iannace[†]

[†]Institute for Composite and Biomedical Materials (IMCB), CNR, P.le Tecchio 80, 80125 Naples, Italy

[§]Department of Materials and Production Engineering, University of Naples Federico II, P.le Tecchio 80, 80125 Naples, Italy

[#]IMAST S.C.aR.L., P.le E. Fermi 1, loc. Granatello, 80055 Portici (Na), Italy

ABSTRACT: The effect of alkaline lignin (AL) and sodium lignosulfonate (LSS) on the structure of thermoplastic zein (TPZ) was studied. Protein structural changes and the nature of the physical interaction between lignin and zein were investigated by means of X-ray diffraction and Fourier transform infrared (FT-IR) spectroscopy and correlated with physical properties. Most relevant protein structural changes were observed at low AL concentration, where strong H-bondings between the functional groups of AL and the amino acids in zein induced a destructuring of inter- and intramolecular interactions in α -helix, β -sheet, and β -turn secondary structures. This destructuring allowed for an extensive protein conformational modification which, in turn, resulted in a strong improvement of the physical properties of the bionanocomposite.

KEYWORDS: bionanocomposites, FT-IR spectroscopy, lignin, zein, X-ray diffraction

INTRODUCTION

The use of natural polymers for the production of plastics is a promising approach for substituting oil-based polymers and is steadily growing.¹ Polymers directly extracted from biomass such as polysaccharides and proteins, besides the natural origin, have the additional advantage of being biodegradable and/or compostable under specific environmental conditions. However, when compared to oil-based polymers, they are inferior in terms of processing and functional and structural performances. In particular, processing problems are mainly due to reduced plastic flow properties of these polymers² and the intrinsically difficult reproducibility and control over the molecular architecture and spatial conformation of natural macromolecules.³ Furthermore, attempts to make plastics from plant materials had the vicious effect of increasing food prices. One alternative is the use of biological feedstocks that are the byproduct of the food and agricultural industries, such as corn zein, wheat gluten, feather keratin, egg albumin, and lactalbumin.⁴

Zein is found in corn endosperm and has been the object of research as well as industrial interest (being commercially available since 1938⁵) for its film-forming ability and its unique hydrophobicity, which is due to its high content of nonpolar amino acids. Like any other protein, upon isolation from the native state, zein shows high density and brittle behavior, with a high modulus and stress to break and a low strain to break. One popular method for utilizing zein is, then, to plasticize it with small polar molecules such as water, glycerol, and ethylene glycol. In this way, although the molecular rearrangement is not regained, some level of plasticization, mimicking natural hydration, allows for a certain polymer flexibility. A reduction in the protein–protein hydrogen-bonding interactions and an increase of free volume and molecular mobility are the possible mechanisms proposed in the literature for describing the effects induced by the presence of the plasticizer. As a matter of fact, the protein amino acids sequence (primary structure) and molecular

architecture, its spatial arrangement (secondary and higher order structure), the intermolecular interactions, and the interactions with the plasticizer are responsible for the definition of the final properties of the natural plastic system.

Recently, the combination of proteins and inorganic solids of at least one characteristic dimension of the order of nanometers (e.g., clays) has become an emerging group of hybrid materials, namely, bionanocomposites. Clay has been successfully used as a nanoscaled reinforcing phase for a wide range of commodity and natural polymers. Some natural polymer/clay materials with high performance such as mechanical, thermal, and barrier properties have been achieved by several research groups. Potentials and problems associated with the use of nanoscaled additives to biopolymers for food packaging applications have been recently reviewed.^{6–8} To have improved properties, dispersion of nanometric additives in the natural polymeric matrix is a key feature and is achieved via the control of the possible interactions between the surface of the nanometric additive and the hydrophobic and/or hydrophilic domains of the molecule. The conformation of the natural polymer itself in the bionanocomposite is, in turn, affected by the presence of the nanometric additive, which, together with the plasticizer and, of course, processing, plays an additional role in defining the final macromolecular conformation. Possibly, for this reason, the final material performances of the bionanocomposites are affected by the presence of the nanometric additive to a more profound extent than in the case of commodity plastics.

In the very recent literature about biopolymers, the control over inter- and intramolecular weak interactions, which play a profound role in defining the performances of the materials because they are responsible for the arrangement at the

Received: May 3, 2011

Revised: August 10, 2011

Accepted: August 11, 2011

Published: August 11, 2011

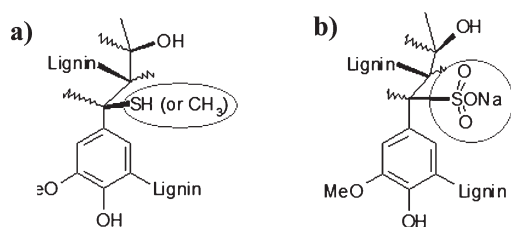


Figure 1. (a) Alkali lignin (AL) and (b) lignosulfonic acid sodium salt (LSS).

macromolecular level (protein conformation), is referred to as supramolecular design. By programming weak forces such as H-bondings, hydrophobic interactions, and ionic interactions, biopolymers may achieve mechanical properties that synthetic polymers still cannot rival.⁹

Lignin is one of the most abundant organic substances on earth, and large amounts are easily available from, for example, bioethanol production.¹⁰ Lignin is primarily a structural material adding strength and rigidity to cell walls and constitutes between 15 and 40% of the dry matter of woody plants. Lignin in the scientific literature is known as “insoluble plant polymer” with aromatic and highly cross-linked structure. From the chemical point of view, lignin can be defined as a very reactive macromolecular compound, because of its functional groups such as aromatic rings, phenolic and aliphatic alcohol groups, and methoxy groups that are possible sites for chemical modification and/or reaction. For this reason, lignin is able to interact with many polymers, by inducing relevant changes in their wettability, fire resistance, and mechanical properties.^{11–13} However, the complexity of the possible chemical interactions between lignin and polymers (in particular, natural polymers) remains, nowadays, an important challenge. In particular, several authors^{11–13} investigated the effect of lignin–natural polymer interactions on the functional and mechanical properties of natural polymers. In these studies, the variation/improvement of the characteristic is strongly dependent upon the chemical functional groups of both lignin (alkaline lignin and lignosulfonate) and natural polymers (soy protein, starch, and others).

In this work, we utilized lignin as a highly interactive additive in thermoplasticized zein to gain a supramolecular control over the structure of zein and, in turn, produce a true bionanocomposite. To this aim, we investigated the effect of two kinds of lignin on the structural arrangement of the protein as well as on the final dynamical mechanical, water absorption, and mechanical properties. The structural investigation has been performed via Fourier transform infrared (FT-IR) and X-ray diffraction (XRD) analyses, which highlighted the changes induced in the α -helix, β -sheet, and β -turn structures of zein.

MATERIALS AND METHODS

Materials. Maize zein powder (code Z3625, lot 065K0110) was purchased from Sigma-Aldrich, Italy. Poly(ethylene glycol), PEG ($M_w = 400$, code 81170, Sigma-Aldrich, Italy) was used as plasticizer for zein to prepare thermoplastic zein (TPZ). To investigate the effect of lignin on zein structure, two different ligninic systems were used, alkali lignin (average $M_w = 28000$ ca., code 370959, Sigma-Aldrich, Italy), hereafter denoted AL, and lignosulfonic acid sodium salt (average $M_w = 52000$ ca., code 471038, Sigma-Aldrich, Italy), hereafter denoted LSS, with two different functional groups (see Figure 1). All of the materials were used as received from the suppliers.

Table 1. Classification of TPZ-Based Nanocomposites

TPZ-based composite	AL (wt %)	LSS (wt %)
TPZ	0	0
TPZ–1AL	1	
TPZ–3AL	3	
TPZ–5AL	5	
TPZ–10AL	10	
TPZ–1LSS		1
TPZ–3LSS		3
TPZ–5LSS		5
TPZ–10LSS		10

Methods. *TPZ-Based Nanocomposites Preparation.* TPZ–AL nanocomposites were prepared by using a melt mixing method. AL was first added to PEG in amounts such that the final concentrations of AL were 1, 3, 5, and 10 wt % of zein+PEG system. The PEG+AL mixture was magnetically stirred in a beaker at room temperature for 3 min to allow a good dispersion of AL into the plasticizer. Subsequently, zein powder (moisture content, as determined by thermogravimetric analysis, equal to 7 ± 0.3 wt %) was added into the PEG+AL system and mixed in a beaker using a spatula to provide a crude blend. The amount of PEG was 25 wt % of the zein+PEG system. The crude blend was then subjected to temperature and shear stresses in a twin counter-rotating internal mixer (Rheomix 600 Haake, Germany) connected to a control unit (Haake PolyLab QC) for thermoplasticization. Mixing temperature, speed of rotation, and mixing time were 70 °C, 50 rpm, and 10 min, respectively.³ Finally, the molten composites were extracted from the mixer and compression molded at 70 °C and 5 MPa into slabs with a thickness of 1 mm by a hot press (P300P, Collin, Germany). The same procedure was used to produce the bionanocomposites with LSS in place of AL. Neat TPZ was subjected to the same mixing procedure for proper comparison. The classification adopted for samples is reported in Table 1.

TPZ-Based Nanocomposites Characterization. Because the use of lignin has been proposed to improve mechanical properties and water sensitivity of TPZ, the effects of different contents of AL and LSS on the structure and properties (mechanical, dynamic mechanical, and water uptake) of TPZ-based nanocomposites were investigated and compared with neat TPZ. Knowledge of the structure of different nanocomposites supports the understanding of the changes occurring in composites' properties. In particular, the crystalline phase (α -helix) of TPZ was investigated by wide angle XRD.¹⁴ FT-IR was used to investigate the effects of lignin on the secondary structure (α -helix, β -sheet, and β -turns) of TPZ.

XRD. The X-ray patterns of the different bionanocomposites were obtained by using a diffractometer PW1710 (Philips, The Netherlands) with a nickel-filtered Cu K α radiation of wavelength 1.54 Å at a voltage of 40 kV and a current of 20 mA. Samples were examined in a range of diffraction angles, $2\theta = 3–60^\circ$, at a scanning rate of $0.6^\circ/\text{min}$ with $0.01^\circ/\text{s}$ steps. XRD signals were deconvoluted with OriginPro 8.0 software by using Lorentzian sum fitting.

FT-IR. FTIR measurements were carried out at room temperature by using a Nicolet apparatus (Thermo Scientific, Italy) and selecting a wavenumber resolution of 4 cm^{-1} for 64 scans from 4000 to 600 cm^{-1} . The FTIR spectra were collected in absorbance mode on transparent pellets obtained by dispersing the sample in the form of powder in KBr (2 wt %/wt). To estimate the content of the various secondary structures, the absorption of the amide I band¹⁵ in the range $1800–1600\text{ cm}^{-1}$ was used. The spectral region analyzed was deconvoluted with OriginPro 8.0 software by using the best fits by Lorentzian sum and specifying the positions of the peaks corresponding to the different conformations (α -helix, β -sheet, and β -turns)¹⁵ in secondary structures.

Dynamic Mechanical Analyses (DMA). Dynamic mechanical tests were carried out by means of a DMA Tritec 2000 (Triton, U.K.) in tensile deformation. Temperature scan tests were performed by applying a tensile amplitude of 10 μm at 1 Hz frequency and at heating rate of 3 $^{\circ}\text{C}/\text{min}$ from -80 to 100 $^{\circ}\text{C}$. The samples sizes were 20 mm long, 8 mm wide, and 0.5 mm thick, and the gauge length was 10 mm.

Sample Conditioning and Water Uptake. Rectangular samples (2 mm \times 1.5 mm \times 0.2 mm), previously dried overnight at 50 $^{\circ}\text{C}$, were weighed and conditioned in a desiccator at 50% relative humidity (RH) and ambient temperature using a saturated salt solution. The amount of water absorbed by the samples was determined by weighing them periodically until a constant weight was attained (indicating water uptake, WU). These experiments were performed in triplicate. The WU of the samples was calculated as¹⁶

$$\text{WU (\%)} = \frac{M_t - M_0}{M_0} \times 100$$

where M_t is the weight at time t and M_0 is the dry weight before exposure to 50% RH.

Tensile Tests. Tensile tests were performed at room temperature according to ASTM standard D1708-02 by using a 4204 Universal Testing Machine (Instron, USA) equipped with a 1 kN load cell. Force and displacement were measured by the apparatus and recorded to evaluate maximum stress (σ_M) and elongation at break (ϵ_B). Five samples for each composition were tested, and the average values were reported. Because the mechanical properties of these materials are known to be strongly affected by water content, samples were preconditioned at room temperature and 50% RH for 48 h before testing.

RESULTS AND DISCUSSION

XRD. As reported by Oliviero et al.,³ the XRD diagram of zein and TPZ typically shows two peaks, at $2\theta = 9.5$ and 20° , which correspond to two characteristic d -spacings around 4.6 \AA (d_0) and 8.96 \AA (d_i) and which are generally attributed to the average backbone distance within the α -helix structure of TPZ and the spacing of α interhelix packing, respectively.^{14,16–18} TPZ-based bionanocomposites containing AL or LSS show similar peaks, but with different peak areas and d -spacings, suggesting possible TPZ organization changes in the presence of lignin.¹⁸ The parameter used to evaluate possible structural changes of TPZ was the area ratio of both peaks (A_i/A_0), as measured from deconvoluted XRD patterns (the 2θ values corresponding to d -spacings at 4.6 \AA , d_0 , and 8.96 \AA , d_i , were used in the Lorentzian fit procedure as input data), as reported by Wang et al.¹⁸ The d -spacings for different TPZ-based nanocomposites as a function of lignin (AL or LSS) content are summarized in Table 2, and the corresponding area ratio A_i/A_0 are given in Figure 2. Both systems showed a decrease of A_i/A_0 with increasing lignin content up to 3 wt %. Because the average backbone α -helix structure (d_0) in zein is stable and not easily changed,¹⁸ this decrease of the area ratio should be attributed to a disruption phenomenon of interhelix packing (d_i).¹⁹ These results suggest that, at these low percentages, both lignins induce a new arrangement of interhelix packing of zein¹⁴ with an insertion of the lignin macromolecule within the layers (see schemes reported in Figure 3a). This arrangement could be induced by the formation of the hydrogen bonding between the amino acids of zein (C=O, OH, RNH) and the functional groups (OH, SH) of lignin fragments, favored by the hydrogen bonding between α -helices in the secondary structure of the protein. An analogous effect in α -zein treated with oleic acid was observed by Wang et al.¹⁸ The authors justified their results by citing the higher

Table 2. X-ray d -Spacings and Glass Transition Temperatures for Neat TPZ and TPZ-Based Nanocomposites

TPZ-base composite	d_0^a (\AA)	d_i^a (\AA)	T_g^b ($^{\circ}\text{C}$)
TPZ	4.6	8.3	46.1
TPZ–1AL	3.9	11.3	42.2
TPZ–3AL	4.6	10.0	37.8
TPZ–5AL	4.6	9.6	53.0
TPZ–10AL	4.5	8.6	45.6
TPZ–1LSS	4.6	9.2	40.1
TPZ–3LSS	4.6	9.3	39.5
TPZ–5LSS	4.6	9.5	50.4
TPZ–10LSS	4.6	8.2	44.0

^aSamples were analyzed in triplicate. Standard deviation of 0.1.

^bSamples were analyzed in triplicate. Standard deviation of 1 $^{\circ}\text{C}$.

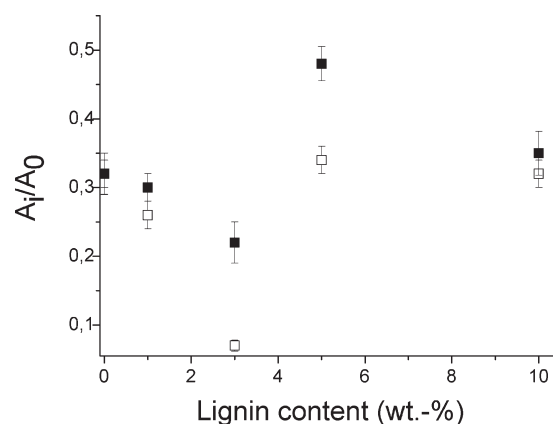


Figure 2. Peak area ratio A_i/A_0 as a function of lignin content (□, AL; ■, LSS) for different TPZ-based nanocomposites.

affinity of zein with polar surfaces, as observed elsewhere.^{20,21} At higher lignin content (starting from 5 wt %), the A_i/A_0 values for TPZ-based bionanocomposites with AL were close to or slightly higher than that of TPZ, suggesting the existence of a certain degree of phase separation between the ligninic-rich phase and the zein phase.¹² This implies that higher contents of lignin were not able to modify the hierarchical structure of the protein in TPZ. Similar results have been observed by Wei et al. for soy protein based plastics filled with lignin.¹⁴ The A_i/A_0 value of TPZ–5LSS was higher than that of neat TPZ; this behavior is related to an increase of α interhelix packing order (because the α -helix structure zein is stable¹⁸) promoted by the interaction with LSS at 5 wt %.¹¹ Another interesting feature is that, at 1 wt % of AL, there was a decrease of d_0 -spacing (see Table 2). This evidence suggested that (only) at this concentration is the AL able to modify the α -helix backbone. This effect could be induced by the formation of strong hydrogen bonding between the amino acids of zein and the SH group (mainly) present in AL. Such strong interactions do not form in samples containing LSS lignin because of the absence of SH groups, which results in unchanged d_0 -spacing.

FT-IR. As described under Materials and Methods, the measured FT-IR spectra were deconvoluted in the region (1800–1600 cm^{-1}) related to the amide I frequency range²² to evaluate possible changes in zein secondary structure induced by the presence of the different contents of AL and LSS. In this

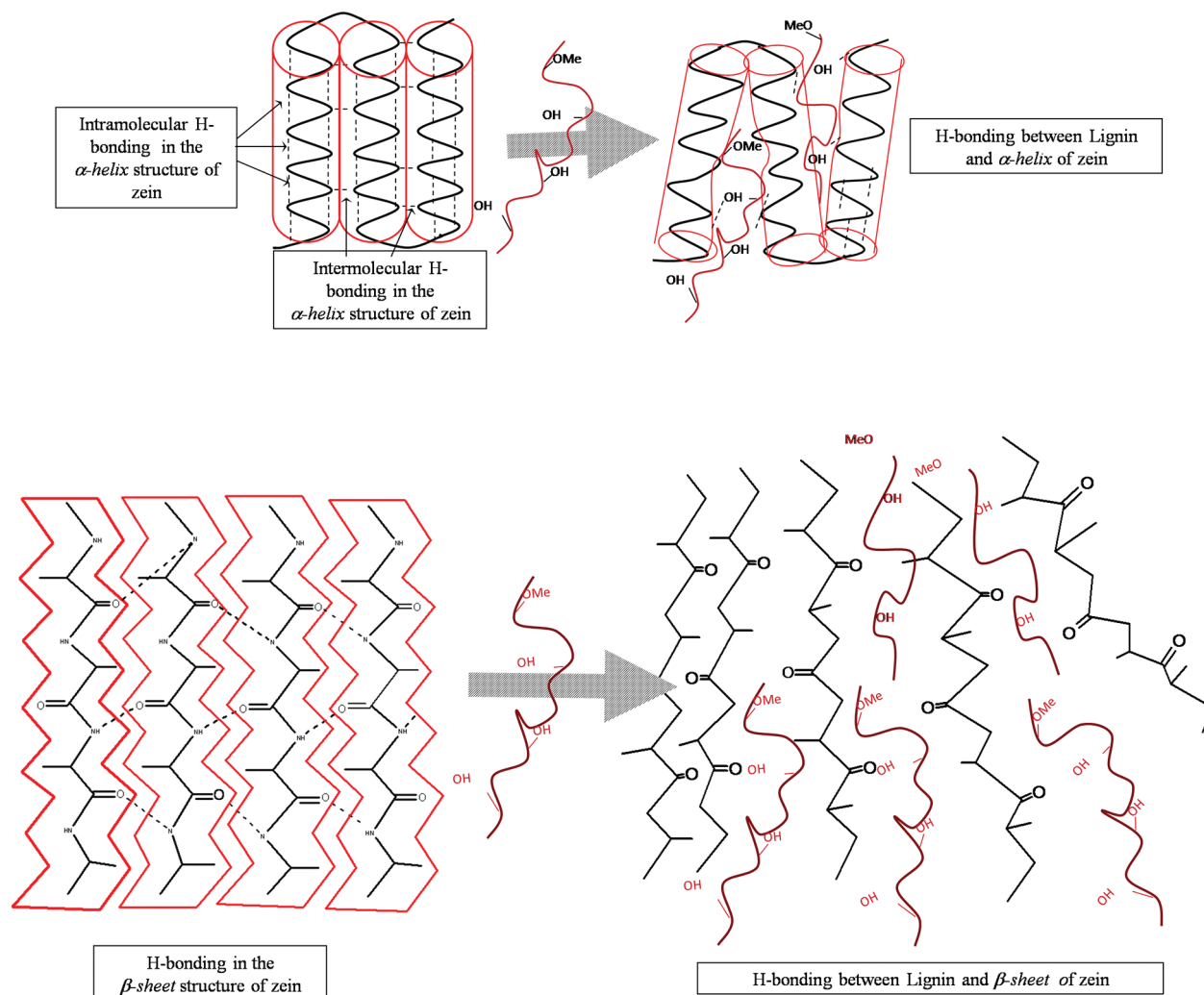


Figure 3. Proposed mechanism of interaction between lignin and different secondary structures of zein: (a, top) α -helix; (b, bottom) β -sheet.

region, the assignment of the β -sheet, α -helix, and β -turn stretching vibrations at 1623, 1651, and 1676 cm^{-1} , respectively, was done according to refs 3 and 19. The deconvolutions of the analyzed spectral region for TPZ-based composites with AL or LSS are reported in Figure 4. Results show that the presence of both AL and LSS induced both shifting in frequencies and changes of band area corresponding to the different secondary conformations (β -sheet, α -helix, and β -turn). In particular, the effects of lignin content (AL and LSS) on amide vibration peaks are detailed in Figure 5 (as suggested by Athamneh et al.,⁴ the α -helix and β -sheet conformations are considered as “ordered” phases, whereas β -turns are “disordered” phases). In Figure 5, it is possible to observe an overall shift toward lower vibration frequencies for ordered conformations with the increase of lignin content to 3 wt % content (both LSS and AL) and a corresponding shift toward higher frequencies of disordered conformations. The shift toward lower frequencies could be attributed to the formation of hydrogen bondings between amino acids of zein and functional groups of lignin, which are favored with respect to the α -helix/ α -helix and β -sheet/ β -sheet hydrogen bondings (see the schemes reported in Figure 3), as already discussed in the previous section. Moreover, for the TPZ-IAL and TPZ-3AL composites, it is possible to observe that the β -sheet

absorption peak disappeared, suggesting that, for these concentrations, the β -sheet aggregates were totally disrupted. The reduction, in the secondary structures, of protein–protein hydrogen bondings induced by small polar molecules (i.e., water, ethylene glycol, glycerol) has been already observed.^{4,23} In particular, Athamneh et al. and Gao et al. noted that, by increasing the glycerol content, the protein–protein hydrogen interactions decreased and glycerol–protein interaction occurred, whereas, at higher glycerol concentrations, the glycerol–glycerol and protein–protein interactions were again favored. In fact, we also observed an increase of peak wavenumber for ordered conformations and a decrease of peak wavenumber for disordered conformations with the increase of lignin content above 5 wt % (Figure 5). An overall description of the relative content of “ordered” and “disordered” conformations can be drawn by reporting the ratio of β -sheet + α -helix/ β -turns ($R = \beta\text{-sheet} + \alpha\text{-helix}/\beta\text{-turns}$) (Figure 6). It is possible to observe that the presence of lignin determined a sharp reduction of this ratio with respect to neat TPZ, proving a strong effect on the protein overall structure. In particular, the lowest value of R is attained when 3 wt % of lignins is used. In summary, the lignin content influenced in different ways the arrangements of secondary structure of zein in TPZ. In particular, we

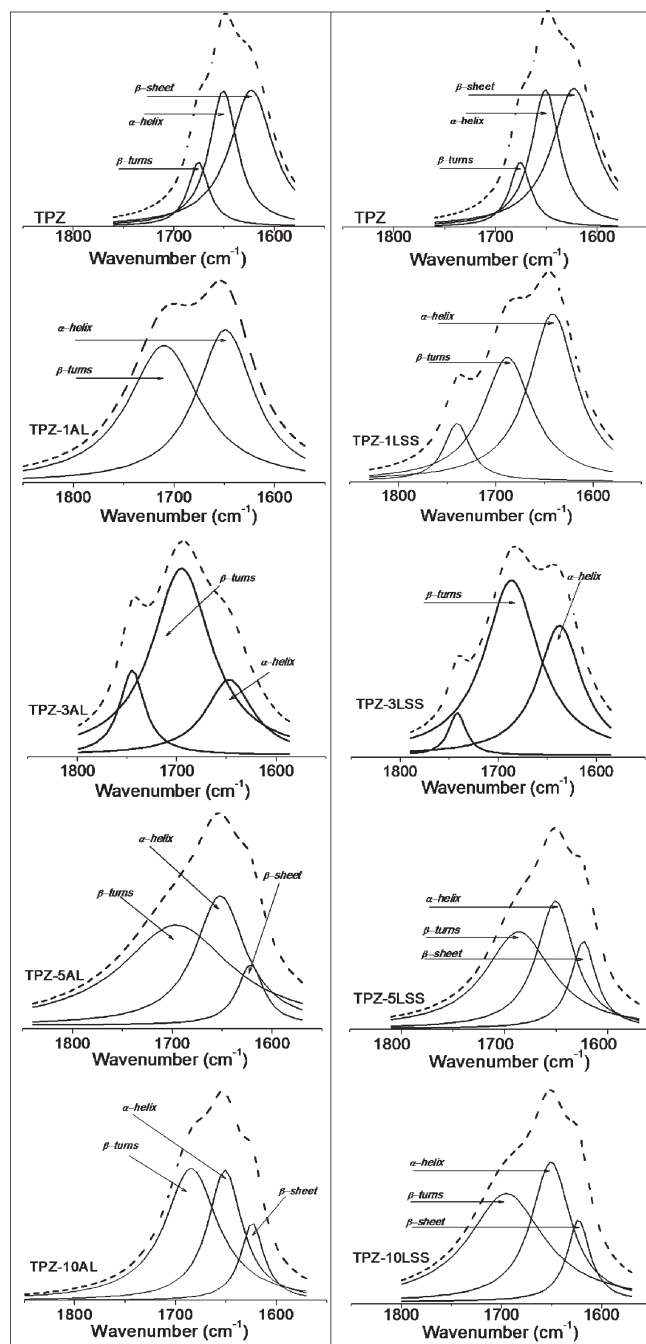


Figure 4. Deconvoluted spectra (solid lines, α -helix, β -sheet, β -turns) and reconstituted spectra after fitting (dashed lines) in the amide I region of neat TPZ and TPZ-AL and TPZ-LSS nanocomposites.

hypothesized that, at lower concentrations (especially 1 wt %) of lignins specific functional groups are able to create strong hydrogen bonding with the polar group of amino acids in the zein protein, thereby inducing new arrangements of the whole secondary structure.

DMA. The thermomechanical properties of neat TPZ and TPZ-based nanocomposites were analyzed by DMA. Figures 7 and 8 show the temperature dependence of storage modulus, E' , and loss tangent, $\tan \delta$, for TPZ-based composites with AL and LSS, respectively. All samples pass through the glassy region, the glass transition region ($\tan \delta$ peak and modulus decrease) and

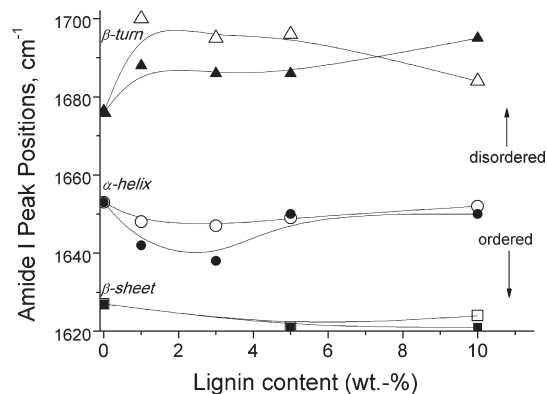


Figure 5. Amide I peak positions in the FT-IR spectra of nanocomposites TPZ-AL (\square , \circ , \triangle) and TPZ-LSS (\blacksquare , \bullet , \blacktriangle) (the lines are guide to the eye only).

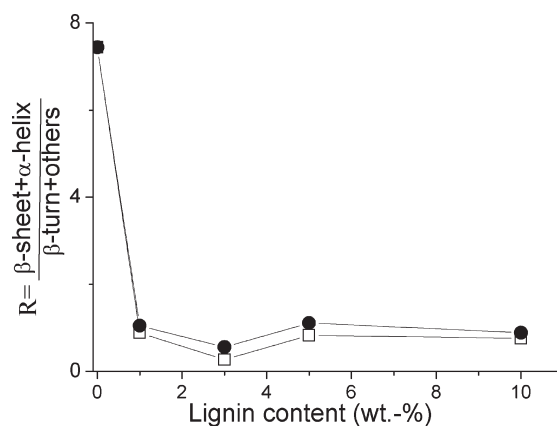


Figure 6. Effect of lignin content (\square , AL; \bullet , LSS) on the ratio R of peak areas of order and disorder phases of TPZ secondary structure.

the rubbery region, with the temperature rise. In biopolymers, the transition from a rigid to a rubbery structure is usually associated with the main α -relaxation phenomenon, which is considered to be equivalent to the glass transition.^{24,25} The glass transition temperatures of samples, T_g , determined as the temperature corresponding to the maximum of the $\tan \delta$ peak,²⁴ are reported in Table 2. The addition of lignin in different amounts (AL and LSS) induced significant changes in the thermomechanical properties of TPZ, mainly in the glass transition region (see Figures 7 and 8), and two cases, as discussed above, can be distinguished: low (1 and 3 wt %) and high (5 and 10 wt %) lignin content. In particular, at low lignin (AL and LSS) content, samples presented a remarkable decrease of the E' values in the glass transition region with respect to neat TPZ, and a corresponding shift of T_g toward lower temperatures, in addition to an increase in the height of the $\tan \delta$ peak. In view of the results from FT-IR and XRD analyses, these trends are governed by the reduction of hydrogen bondings in secondary structure of the zein as a consequence of modification of α -helix structure and the disruption of the β -conformation through the insertion of the lignin (see Figure 3). As also reported by Mizuno et al.,²⁶ the intermolecular interactions may prevent the local molecular motion; therefore, when these interactions are reduced, the mobility of TPZ-based nanocomposites might increase with a corresponding decrease in T_g . In particular,

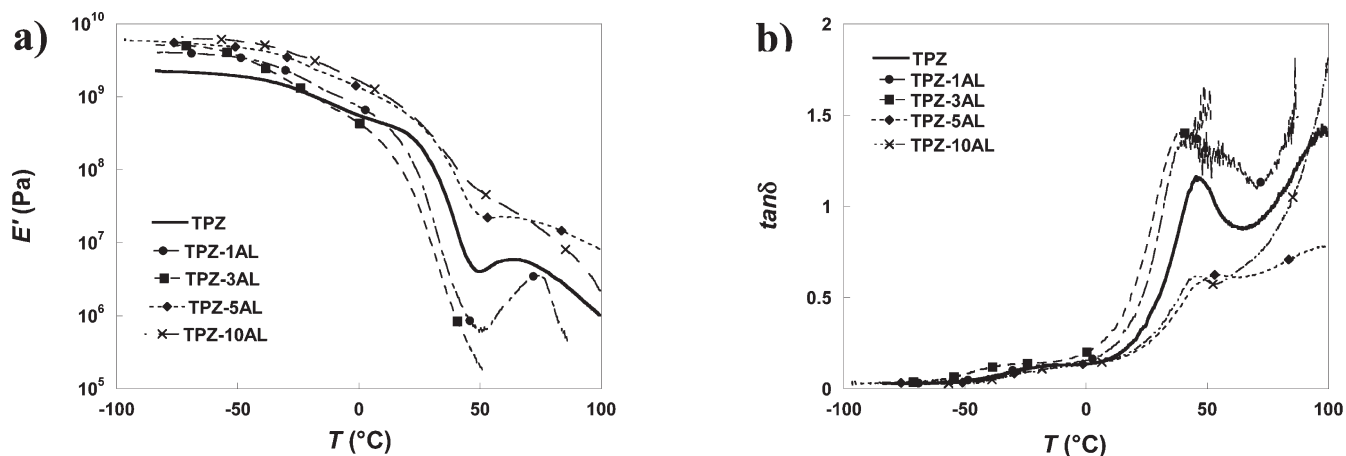


Figure 7. Temperature dependence of storage modulus E' (a) and loss tangent $\tan \delta$ (b) for neat TPZ and TPZ–AL nanocomposites.

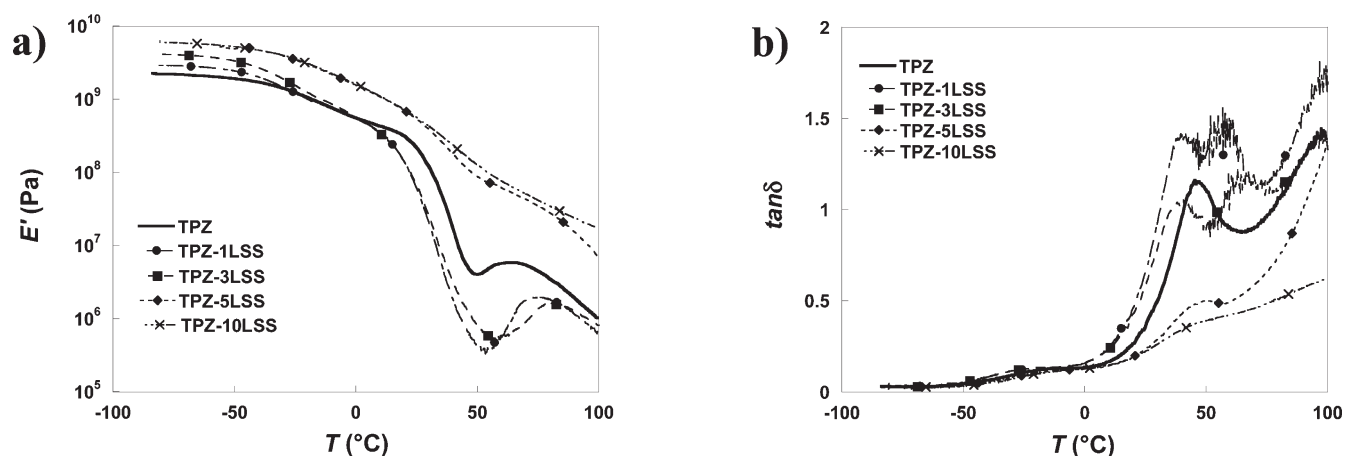


Figure 8. Temperature dependence of storage modulus E' (a) and loss tangent $\tan \delta$ (b) for neat TPZ and TPZ–LSS nanocomposites.

authors related T_g depression of soy proteins cross-linked by microbial transglutaminase (MTG) treatment to the modification of the state of the secondary structure of the protein, especially to the disruption of the β -structure induced by MTG treatment.

Furthermore, the decrease in storage modulus at T_g of low lignin content samples is >3 orders of magnitude (Figures 8 and 9), analogous to amorphous polymers from fossil resources,²⁷ in agreement with the reduced order in secondary structures with respect to neat TPZ. Conversely, high lignin content samples presented a decrease in storage modulus at $T_g < 2$ orders of magnitude (Figures 8 and 9), showing a behavior similar to that of cross-linked systems or semicrystalline polymers with high degrees of crystallinity,^{24,27} due to a high number of interactions between zein structure and lignin functional groups.

Water Uptake. Water uptake values of TPZ-based nanocomposites with LSS and AL are presented in Figure 9 and compared with neat TPZ. As expected, the presence of LSS did not reduce the water sensitivity of TPZ, because the sulfonic acid groups of LSS are hydrophilic. Conversely, the introduction of hydrophobic AL efficiently restricted the water uptake, especially at an AL content of 1 wt %. This is a consequence of the interactions taking place at this AL concentration between the hydroxyl groups of zein and OH and/or SH groups of AL, which led to a significant decrease in the concentration of hydrophilic amino

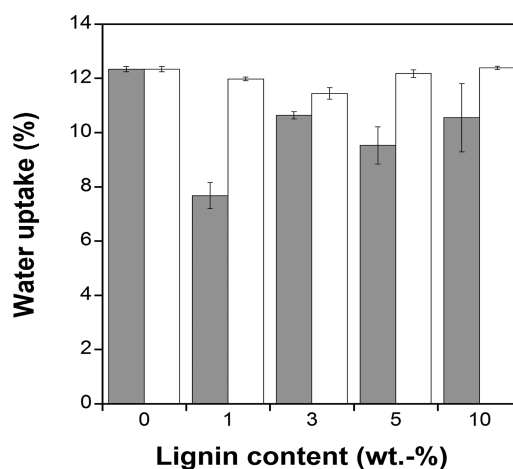


Figure 9. Water uptake (percent) at 50% RH for TPZ and TPZ-based nanocomposites with AL (gray bars) and LSS (white bars).

acids residues in zein and resulted in reduced sorption sites for water molecules, as also reported by Talja et al.²⁸

Mechanical Properties. The effects of the lignin content on σ_M and ϵ_B for the neat TPZ and TPZ-based nanocomposites with AL and LSS are shown in Figure 10, panels a and b,

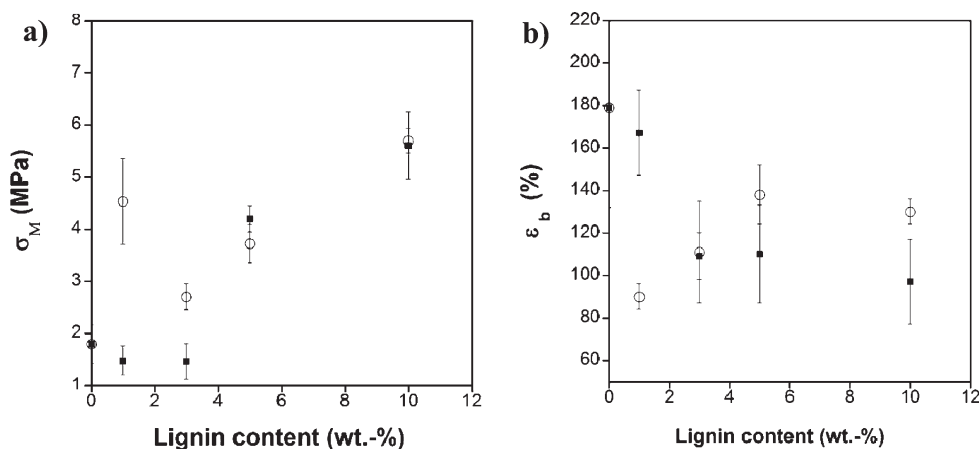


Figure 10. σ_M (a) and ϵ_B (b) of TPZ-based nanocomposites as a function of AL (○) and LSS (■) content.

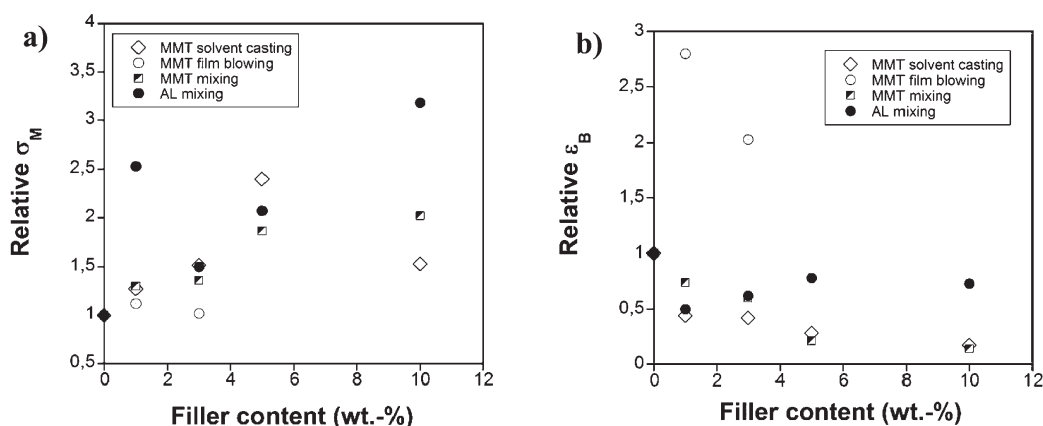


Figure 11. Relative σ_M (a) and relative ϵ_B (b) of zein-based nanocomposites as a function of filler content.

respectively. The value of σ_M increased with AL content, and a significant improvement was observed, in particular, at low AL content (1 wt %). The σ_M increased by about 150% from 1.79 MPa for neat TPZ to 4.53 MPa for the TPZ–1AL bionanocomposite. However, a further increase of AL content resulted in a slight decrease of the σ_M . Conversely, the percentage elongation at break values showed a slight decrease as the AL content increased. A significant reduction of this property was observed only when the content of AL was 1 wt %. The increase of σ_M and decrease of ϵ_B when the content of AL was 1 wt % can be again attributed to the optimal interaction between lignin and protein molecules, in particular, to the formation of the strong hydrogen bondings between the amino acids of the zein ($-\text{C}=\text{O}$, $-\text{OH}$, $-\text{NH}$) and the functional groups ($-\text{OH}$ and, mainly, $-\text{SH}$) of AL, as already discussed.²⁹ The slight decrease of σ_M of the bionanocomposites when the content of AL exceeded 1 wt % is due to the reduction of the intramolecular interactions, in α -helix conformation, between TPZ and AL as observed in the XRD discussion. At 10 wt %, the AL can be simply considered as reinforcing filler for TPZ. An improvement of the mechanical properties of TPZ–LSS nanocomposites was observed only for LSS content from 5 to 10 wt %. Compared with LSS, AL exhibited a greater reinforcement effect on TPZ, mainly for the presence of SH groups, capable of forming stronger hydrogen bonding rather than simple protein/protein interactions. Similar

results have been reported by Huang et al.^{11,12} on the effect of alkaline lignin and lignosulfonate on properties of soy protein plastics. The authors observed, however, only a 50% increase in σ_M with the addition of 30 wt % lignin. They hypothesized that the observed behavior might have been due to inadequate mixing of lignin with protein and suggested improvement of the affinity of the two phases by using methylene diphenyl diisocyanate as compatibilizer³⁰ or by using a chemically modified lignin.¹⁴ In our work, a remarkable improvement of mechanical properties was observed even at low lignin content (1 wt %). We believe that the PEG in which the lignin has been dispersed reduced the degree of self-association between lignin molecules and favored a good mixing and interaction of AL with zein molecules.³¹ In Figure 11 is reported a comparison among the mechanical properties of TPZ–AL nanocomposites and the mechanical properties of other zein–montmorillonite (MMT) nanocomposites found in the literature, prepared by solvent casting,³² film blowing of a resin obtained by the precipitation of zein from an aqueous ethanol solution,³² and melt mixing⁸ methods. The effect of filler content on σ_M and ϵ_B was expressed as the relative values with respect to the neat system. These data clearly evidence the high efficiencies of AL with respect to MMT, even at very low lignin content (1 wt %).

Conclusions. Two types of lignin (AL, LSS) were blended into TPZ through melt mixing to develop a potential biodegradable

polymer with better mechanical performance than that of neat TPZ. The structure and properties of the composite materials were characterized by XRD, FT-IR, DMA, and mechanical and water absorption tests. The addition of 1 wt % of AL resulted in an improvement of 150% in maximum stress and in a reduction of 33% of water uptake with respect to neat TPZ, as a consequence of the partial disruption of the zein secondary structure (inter/intramolecular interactions in α -helix and β -conformations) induced by strong H-bondings established between the functional groups of AL and the amino acids of zein. As the AL content increased, phase separation occurred in the bionanocomposite because protein–protein interactions were again favored with respect to lignin–protein interactions.

Variation in zein conformations strongly influenced the mechanical and thermal properties of TPZ–AL composites. Dynamic mechanical analysis showed that the addition of lignin into TPZ induced a shift of T_g toward lower temperatures along with a steeper modulus decrease at low lignin concentration, whereas, at high concentrations, the storage modulus drop was less pronounced than that of neat TPZ, with an apparent shift from amorphous-like (low lignin content) to cross-linked-like (high lignin content) polymer behavior. Compared with TPZ–AL bionanocomposites, the TPZ–LSS bionanocomposites presented similar mechanical and thermal properties, even though molecular interactions between LSS and zein were weaker with respect to AL due to different functional groups.

This work proved that, by modifying the hierarchical structure of zein with the use of a highly interactive additive such as lignin, it is possible to achieve a supramolecular design of the protein and obtain bionanocomposites characterized by enhanced mechanical performances and specific functional properties (from hydrophilic to hydrophobic behavior) suitable for specific applications (from biomedical uses to food packaging).

AUTHOR INFORMATION

Corresponding Author

*E-mail: edimaio@unina.it. Phone: +39 081 768 25 11. Fax: +39 081 768 24 04.

Funding Sources

This work was supported in part by the Italian Ministero dell'Istruzione, dell'Università e della Ricerca (MIUR), within the framework of FIRB under Grant RBPR05JH2P "ITALNANONET".

ACKNOWLEDGMENT

We thank Fabio Docimo for technical support in the preparation of TPZ-based bionanocomposites.

REFERENCES

- (1) Mohanty, A. K.; Misra, M.; Drzal, L. T. Sustainable bio-composites from renewable resources: opportunities and challenges in the green materials world. *J. Polym. Environ.* **2002**, *10*, 19–26.
- (2) Di Maio, E.; Mali, R.; Iannace, S. Investigation of thermoplasticity of zein and kafirin proteins: mixing process and mechanical properties. *J. Polym. Environ.* **2010**, *18*, 626–633.
- (3) Oliviero, M.; Di Maio, E.; Iannace, S. Effect of molecular structure on film blowing ability of thermoplastic zein. *J. Appl. Polym. Sci.* **2010**, *115*, 277–287.
- (4) Athamneh, A. I.; Griffin, M.; Whaley, M.; Barone, J. R. Conformational changes and molecular mobility in plasticized proteins. *Biomacromolecules* **2008**, *9*, 3181–3187.

- (5) Lai, H. M.; Padua, G. W. Properties and microstructure of plasticized zein films. *Cereal Chem.* **1997**, *74*, 771–775.
- (6) Lavorgna, M.; Piscitelli, F.; Mangiacapra, P.; Buonocore, G. Study of the combined effect of both clay and glycerol plasticizer on the properties of chitosan films. *Carbohydr. Polym.* **2010**, *82*, 291–298.
- (7) Arora, A.; Padua, G. W. Review: Nanocomposites in food packaging. *J. Food Sci.* **2010**, *75*, R43–R49.
- (8) Mensitieri, G.; Di Maio, E.; Buonocore, G. G.; Nedi, I.; Oliviero, M.; Sansone, L.; Iannace, S. Processing and shelf life issues of selected food packaging materials and structures from renewable resources. *Trends Food Sci. Technol.* **2011**, *22*, 72–80.
- (9) Guan, Z. Supramolecular design in biopolymers and biomimetic polymers for advanced mechanical properties. *Polym. Int.* **2007**, *56*, 467–473.
- (10) Doherty, W. O. S.; Mousavioun, P. C.; Fellows, M. Value-adding to cellulosic ethanol: lignin polymers. *Ind. Crops Prod.* **2010**, *33*, 259–276.
- (11) Huang, J.; Zhang, L.; Chen, F. Effects of lignin as a filler on properties of soy protein plastics. I. Lignosulfonate. *J. Appl. Polym. Sci.* **2003**, *88*, 3284–3290.
- (12) Huang, J.; Zhang, L.; Chen, P. Effects of lignin as a filler on properties of soy protein plastics. II. Alkaline lignin. *J. Appl. Polym. Sci.* **2003**, *88*, 3291–3297.
- (13) Baumberger, S.; Lapierre, C.; Monties, B.; Valle, G. D. Use of kraft lignin as filler for starch films. *Polym. Degrad. Stab.* **1998**, *99*, 273–277.
- (14) Wei, M.; Fan, L.; Huang, J.; Chen, Y. Role of star-like hydroxylpropyl lignin in soy-protein plastics. *Macromol. Mater. Eng.* **2006**, *291*, 524–530.
- (15) Rahmelow, K.; Hubner, W. Fourier self-deconvolution: parameter determination and analytical band shapes. *Appl. Spectrosc.* **1996**, *50*, 795–804.
- (16) Comyn, J. *Polymer Permeability*; Elsevier Applied Science: New York, 1985.
- (17) Arndt, U. K.; Riley, D. P. The structure of some proteins as revealed by an X-ray scattering method. *Philos. Trans. R. Soc. London, A* **1955**, *247*, 409–439.
- (18) Wang, Y.; Filho, F. L.; Geil, P.; Padua, G. W. Effects of processing on the structure of zein/oleic acid films investigated by X-ray diffraction. *Macromol. Biosci.* **2005**, *5*, 1200–1208.
- (19) Yao, C.; Xinsong, L.; Tangyung, S. Preparation and characterization of zein and zein/poly-L-lactide nanofiber yarns. *J. Appl. Polym. Sci.* **2009**, *114*, 2079–2086.
- (20) Forato, L. A.; Yushmanov, V. E.; Colnago, L. A. Interaction of two prolamins with $1\text{-}^{13}\text{C}$ oleic acid by ^{13}C NMR. *Biochemistry* **2004**, *43*, 7121–7126.
- (21) Wang, Q.; Wang, J. F.; Geil, P. H.; Padua, G. W. Zein adsorption to hydrophilic and hydrophobic surfaces investigated by surface plasmon resonance. *Biomacromolecules* **2004**, *5*, 1356–1361.
- (22) Singh, N.; Georget, D. M. R.; Belton, P. S.; Barker, S. A. Physical properties of zein films containing salicylic acid and acetyl salicylic acid. *J. Cereal. Sci.* **2010**, *52*, 282–287.
- (23) Gao, C.; Stading, M.; Wellner, N.; Parker, M. L.; Noel, T. R.; Mills, E. N. C.; Belton, P. S. The plasticization of protein-based film by glycerol: a spectroscopic, mechanical and thermal study. *J. Agric. Food Chem.* **2006**, *54*, 4611–4616.
- (24) Galiotta, G.; Di Gioia, L.; Guilbert, S.; Cuq, B. Mechanical and thermomechanical properties of films based on whey proteins as affected by plasticizer and crosslinking agents. *J. Dairy Sci.* **1998**, *81*, 3123–3130.
- (25) Cuq, B.; Gontard, N.; Guilbert, S. Thermoplastic properties of fish myofibrillar proteins: application to biopackaging fabrication. *Polymer* **1997**, *38*, 4071–4078.
- (26) Mizuno, A.; Mitsuiki, M.; Motoki, M.; Ebisawa, K.; Suzuki, E. Relationship between the glass transition of soy protein and molecular structure. *J. Agric. Food Chem.* **2000**, *48*, 3292–3297.
- (27) Sperling, L. H. *Introduction to Physical Polymer Science*, 4th ed.; Wiley: Hoboken, NJ, 2006.

(28) Talja, R. A.; Helen, H.; Roos, Y H.; Jouppila, K. Effect of various polyols and polyol contents on physical and mechanical properties of potato starch-based films. *Carbohydr. Polym.* **2007**, *67*, 288–295.

(29) Herald, T. J.; Gnanasambandam, R.; Mcguire, B. H.; Hachmester, K. Degradable wheat gluten films: preparation, properties and applications. *J. Food Sci.* **1995**, *60*, 1147–1150.

(30) Huang, J.; Zhang, L.; Wei, H.; Cao, X. Soy protein isolate/kraft lignin composites compatibilized with methylene diphenyl diisocyanate. *J. Appl. Polym. Sci.* **2004**, *93*, 624–629.

(31) Feldman, D.; Banu, D.; Campanelli, J.; Zhu, H. Blends of vinylic copolymer with plasticized lignin: thermal and mechanical properties. *J. Appl. Polym. Sci.* **2001**, *81*, 861–874.

(32) Luecha, J.; Sozer, N.; Kokini, J. L. Synthesis and properties of corn zein/montmorillonite nanocomposite films. *J. Mater. Sci.* **2010**, *45*, 3529–3537.